Frontiers in Heat and Mass Transfer (FHMT), 18, 26 (2022)
DOI: 10.5098/hmt.18.26

Global Digital Central
ISSN: 2151-8629

Frontiers in Heat and Mass Transfer

Available at www.ThermalFluidsCentral.org

SELF-COUPLING NUMERICAL CALCULATION OF CENTRIFUGAL PUMP STARTUP PROCESS

L. Cheng, Y. L. Zhang†

College of Mechanical Engineering, Quzhou University, Quzhou, Zhejiang, 324000, China

ABSTRACT

To obtain the transient characteristics of a centrifugal pump during a rapid startup process accurately, a circulating piping system, including the pump, is established. A full three-dimensional unsteady incompressible viscous flow of a low-specific speed centrifugal pump during rapid startup is numerically simulated using the finite volume method, RNG *k-ε* turbulence model, sliding grid technology, dynamic grid technology, and user-defined function. Results show that the effect of dynamic and static interference becomes remarkably evident with the increase in speed in the starting process. The effect of dynamic and static interference makes the flow rate show small fluctuation characteristics, and the flow rate rises slowly in the initial stage of startup. The evolution of the transient flow field lags behind that of the quasi-steady flow field, which may be related to the fact that the pressure energy is not converted into kinetic energy in time during the transient process. The entire startup process shows evident transient behavior.

Keywords: *Centrifugal pump; Startup; Transient effect; Numerical simulation; Quasi-steady state*

1. INTRODUCTION

The starting process of a centrifugal pump is an essential transient process before normal operation. With the expansion of the application fields of cutting-edge technology, such as underwater weapon launches and rapid startup of large pumping stations, research on such transient performance becomes increasingly necessary. Studies have shown that centrifugal pumps exhibit evident transient effects during transient operation, which are clearly different from those during steady-state processes. Tsukamoto *et al*. (1982, 1986) conducted theoretical and experimental studies on the startup and shutdown processes of a centrifugal pump. The pulse pressure and the delay around the vane are the main reasons for the difference between transient and quasi-steady states. Tsukamoto *et al*. (1995) also performed a study on the transient problem of centrifugal pump speed when the speed of the centrifugal pump changes in a sinusoidal law. In fact, this model is similar to the frequency conversion speed regulation process. The study found that the higher the frequency of the fluctuation in the speed is, the more evident the difference between the transient and quasi-steady states. Lefebvre (Lefebvre and Barker (1995)) conducted an experimental study on four cases of acceleration and deceleration transient processes of a mixed flow pump, and the results showed that the quasi-steady-state hypothesis is unreliable in predicting the transient performance of the pump. Thanapandi (Thanapandi and Prasad (1995)) conducted an experimental study on the transient characteristics of a volute pump at different valve openings under normal startup and shutdown conditions and found that the general transient operation process satisfies the quasi-steady-state assumption. At the same time, they analyzed the transient effect for the first time by using the characteristic method. Dazin *et al*. (2007) proposed the method of using angular momentum and energy equations to predict the internal torque, power, and head of an impeller under transient operating conditions and indicated that the transient effect is related to not only the relatively fixed acceleration and flow rate but also the evolution of flow field. Tanaka *et al*. (1999, 1999, 1999) conducted an experimental study on the cavitation performance of centrifugal pumps during valve closing, valve opening, starting, and stopping. The study found that in the process of closing and adjusting the valve, the unsteady pressure and flow are related to cavitation, and the fluctuation in pressure and flow is related to cavitation fluctuation or water flow separation. Transient behavior is classified in accordance with the increase or decrease in flow. The transient behavior during valve opening and starting is remarkably different from the transient behavior during valve closing and shutdown. Li *et al*. (2010) performed a numerical simulation of the three-dimensional incompressible unsteady viscous flow field of a centrifugal pump in a fast-start transient engineering on the basis of the experimental results in existing literature and used the dynamic grid method; the results proved that the numerical simulation method is completely feasible. Numerical simulationsand experimental studies on the hydraulic characteristics of centrifugal and mixed-flow pumps during startup were carried out by Wu *et al.* (2006), Hu *et al*. (2005), Wang *et al*. (2008), Wu *et al*. (2009), and Zhang *et al*. (2017); they found that the process shows evident transienteffects. Wu *et al*. (2010) conducted numerical simulation and experimental research on the characteristics of a centrifugal pump in the sudden opening condition of the pipeline valve and tested the external characteristics and internal flow field of the centrifugal pump under different stable flow rates. The transient behavior is also found in other flow (Gu *et al*. (2020), Abed *et al*. (2020)).

During the startup process, the speed, flow, and head change rapidly, and they are all functions of time. Therefore, to perform a transient simulation of an isolated pump, at least one of the following two conditions should be known: (1) the relationship between rotation speed and flow rate over time and (2) the relationship between rotation rate and inlet and outlet pressures over time. In short, the functional relationship between speed and time is essential. The change law of speed with time basically does not depend on the pump but directly depends on the characteristics of the power source. In the boundary conditions, the flow rate and inlet and outlet pressures depend on the

† *Corresponding author. Email: zhang002@sina.com*

Global Digital Central
ISSN: 2151-8629

changing law of speed. Consequently, the boundary conditions are difficult to apply accurately. In Literature (Zhang *et al*. (2017)), Zhang et al. established a circulating pipeline system, including a water tank, to calculate the startup process. Compared with the small volume of a pump itself, the volume of a water tank and the number of grids are large, which greatly increases the workload of numerical calculations. The current study includes a centrifugal pump in a circulating pipeline, and the water tank is simplified as a part of the pipeline system, thereby greatly reducing the number of grids and the calculation workload. In Literature (Zhang *et al*. (2017)), the stable flow rate after the startup process is 4.3337 m^3/h; in the current study, the stable flow rate of the model pump in the simplified system is 4.14 m^3/h. Both are in the range of small-flow conditions. As we know, the internal flow field and the external hydraulic performance are different due to the difference in working conditions. In this paper, the calculated object is a closed circulating pipeline system, therefore the numerical calculation does not need to provide redundant boundary conditions so as to realize a self-coupling solution, and the change law of each physical quantity at the inlet and outlet boundaries is calculated through numerical simulation.

2. NUMERICAL SIMULATION METHOD

2.1 Calculation Model

The pump used in the numerical simulation is a centrifugal pump with a low specific speed of 45, and its geometric participation is exactly the same as that in Literature (Zhang *et al*. (2017)). The main design parameters of the centrifugal pump are as follows: a flow of 6 m^3/h, a head of 8 m, and a speed of 1450 r/min. The blade profile adopts a double-arc cylindrical shape, and the volute size change law adopts the Archimedes spiral form.

2.2 Meshing

GAMBIT software is used for meshing, in which the impeller and volute area use an unstructured tetrahedral mesh, and the other calculation domains use a structured hexahedral mesh. The influence of the number of grids on the calculation accuracy is shown in Fig. 1. The circulation piping system, including the centrifugal pump and the grid division of the centrifugal pump, are shown in Fig.2. The role of the throat in the pipeline system is similar to that of a valve. Controlling the diameter of the throat can change the final stable flow. Various valves, water tanks, and pipelines in an actual piping system can be regarded as resistance elements, and they can be replaced with the throat function. On the basis of the correlation check, when the change in the calculated external characteristics is less than 2%, the grid independence requirement is met. In consideration of the computational efficiency, the total number of grids in the final computational domain is set to 641902. The number of grids in the impeller area is 280772, the number of grids in the volute is 191177, and the number of grids in the piping system area is 169953. The number of grids is still slightly insufficient for simulating the flow in the boundary layer, but it is sufficient for the prediction of external characteristics. The grid quality inspection indicates that the equal-angle and -size slopes of the grid are not more than 0.83, which meets the quality requirement that the equiangular and equidimension slopes of the grid should not exceed 0.85.

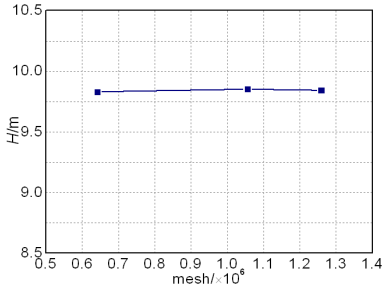

Fig. 1 Independence of the grid number

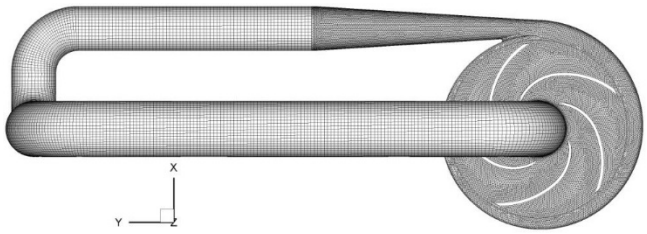

Fig. 2 Computational domain and grid

2.3 Solution Control

The commercial calculation software FLUENT6.3 based on the finite volume method is used for the numerical calculation of full three-dimensional, incompressible, unsteady, and viscous fluids. During the startup process, the Reynolds number changes rapidly from zero to millions, the flow changes rapidly from laminar flow in the initial stage to turbulent flow, and various flow modes change greatly. In this study, the RNG *k*-*ε* turbulence model is used in the eddy viscosity model.

$$\rho\frac{\mathrm{d}k}{\mathrm{d}t}=\frac{\partial}{\partial x_j}\left(\alpha_k\mu_{\mathrm{eff}}\frac{\partial k}{\partial x_j}\right)+2\mu_t\overline{\boldsymbol{S}_{ij}}\frac{\partial\overline{u}_i}{\partial x_j}-\rho\varepsilon \tag{1}$$

$$\rho\frac{\mathrm{d}\varepsilon}{\mathrm{d}t}=\frac{\partial}{\partial x_j}\left(\alpha_\varepsilon\mu_{\mathrm{eff}}\frac{\partial\varepsilon}{\partial x_j}\right)+2C_{1\varepsilon}\frac{\varepsilon}{k}\nu_t\overline{\boldsymbol{S}_{ij}}\frac{\partial\overline{u}_i}{\partial x_j}-C_{2\varepsilon}\rho\frac{\varepsilon^2}{k}-R \tag{2}$$

The speed change of the impeller area is loaded using a user-defined function in the dynamic grid method, and the dynamic and static interference between the impeller and volute is realized using the sliding grid technology. In accordance with existing literature, the change in the motor speed during the startup process increases approximately exponentially (Zhang *et al*. (2017)), as shown as follows:

$$n=n_{\max}(1-e^{-t/t_0}) \tag{3}$$

where $n_{\max}$ is the highest speed, which is 1450 r/min, t_0=0.15s, in this study.

The sliding grid technology can make the grids on both sides of the interface slide each other, without requiring the grid points on both sides of the interface to coincide with each other but requiring the fluxes on both sides of the interface to be equal. When the sliding grid transfers data through the interface, the grid does not need to be reconstructed. After each time step iteration, the entire sliding area moves in a specified manner to perform the iterative calculation of the next time step.

In consideration of viscosity, the nonslip boundary condition is adopted at the wall, and the standard wall function method is used in the low-Reynolds number area near the wall to deal with the problems caused by the high-Reynolds number turbulence model. The time discretization of the transient term adopts the first-order implicit format, the spatial discretization of the convection term adopts the first-order upwind style, the spatial discretization of the diffusion term adopts the central difference format with second-order precision, and the spatial discretization of the source term adopts the linear standard format. The coupling of speed and pressure is realized using the SIMPLE algorithm. All variables in the iterative calculation adopt the default under-relaxation factor. The time step is regarded as 0.0001 s, and the startup time is 1.0 s. The maximum number of iterations is set to 1000 times in each time step (actually, it can be converged by iterating dozens of times in each time step) to ensure absolute convergence in each time step. The convergence residual of the continuity equation is 0.0001, and the convergence residual of the momentum equation is 10^{-7}.

Global Digital Central
ISSN: 2151-8629

3. RESULT ANALYSIS

3.1 External Characteristic Prediction

In consideration of the effect of inertia, the head of the centrifugal pump at any time during startup is composed of basic and inertial heads. With the help of numerical calculation, the expression of head is

$$H = \frac{P_o - P_i}{\rho g} + \frac{Q^2}{2g}\left(\left(\frac{4}{\pi d_o^2}\right)^2 - \left(\frac{4}{\pi d_i^2}\right)^2\right) + \left(\frac{L_{eq}}{gA_0}\right)\frac{dQ}{dt} \quad (4)$$

The last term in the above formula is the inertia term, L_{eq} is the equivalent length of the circulating pipeline, and the calculation method has been provided in Literature (Tsukamoto and Ohashi (1982)). A_0 is the average cross-sectional area of the equivalent pipeline. P_i and P_o are the static pressures in the flow section of the pump inlet and outlet, respectively; and d_i and d_o are the diameters of the pump inlet and outlet, respectively. The model pump in this study is a low-specific speed centrifugal pump with a small flow rate, such that the inertial head caused by the inertial action can be ignored.

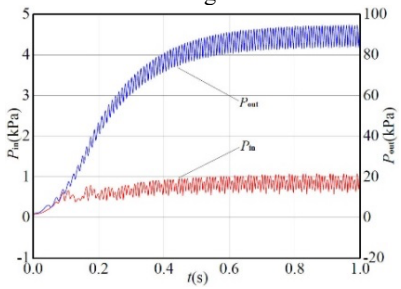

(a)Total pressure of import and export

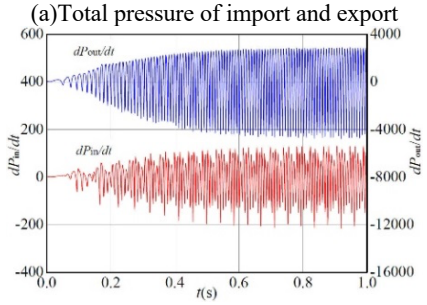

(b)Time change rate

Fig. 3 Rising characteristics of total pressure at inlet and outlet

Figure 3(a) is the temporal course of the instantaneous relative total pressure change in the inlet and outlet overcurrent section during the startup process, with a similar overall evolution trend to that in Literature (Zhang *et al*. (2017)). With the continuous increase in speed during the startup process and the action of the impeller, the outlet pressure increases rapidly. The higher the speed is, the greater the outlet pressure fluctuation will be, which is caused by the inherent dynamic and static interference effects in the pump. Therefore, the dynamic and static interference effect in fluid machinery becomes increasingly evident with the increase in speed. When the startup time t <0.5 s, the speed is rising. The speed rise has been completed by more than 95% by 0.5 s, and the law of outlet pressure rise is similar to the law of speed rise. At 0.5 s< t <1.0 s, the outlet pressure also rises slowly with the slow rise in speed. Before reaching a stable speed, the maximum fluctuating pressure can reach 11 kPa, which accounts for approximately 13% of the average outlet pressure. Consequently, the effect of dynamic and static interference on the low-lift pump will be remarkably evident. When the startup time t <0.2 s, the speed is rising rapidly, the inlet pressure fluctuates greatly, and the fluctuations are irregular. At approximately 0.2 s< t <0.5 s, the speed rises slowly, and the inlet pressure rises in a regular fluctuation pattern because of dynamic and static interference. At 0.5 s< t <1.0 s, the speed is rising slowly, the inlet pressure presents a periodic fluctuation, and the average value is almost unchanged.

Figure 3(b) shows the time derivative of the total inlet and outlet pressure during the startup process. At t <0.1 s, the time derivative of the total inlet pressure is approximately a constant, indicating that the inlet pressure shows an approximately linear upward trend. At approximately 0.4 s, the dynamic and static interference effect shows standard periodic fluctuation characteristics. At t <0.05 s, the time change of the total outlet pressure is not dramatic, which is also approximately a constant. At 0.05 s< t <0.6 s, the effect of dynamic and static interference increases the degree of fluctuation with time, indicating that the real fluctuations are intense. At approximately 0.6 s, the periodic fluctuation characteristics basically no longer change, that is, the fluctuations are stable.

Figure 4 is the temporal course of the head and flow change during the startup process obtained through numerical calculation. With the continuation of the startup time, the rising law of the head shows the same trend as the outlet pressure of the pump. The outlet pressure is much greater than the inlet pressure at any time, and the pump head is mainly determined by the outlet pressure. With the continuous increase in speed, the fluctuation in head becomes remarkably evident, that is, the effect of dynamic and static interference intensifies. The change law of flow and head is consistent with the law of speed increase; in essence, both are directly determined by speed. The time rate of change in flow rate and rotation speed shows a considerable difference. The law of head change over time is similar to that of the outlet pressure because the outlet pressure mainly determines the pump head. Although the calculation model is simplified and the calculation workload is reduced, the physical model of the pump in this paper is unchanged, and the same speed-rising law is adopted during the startup process; as a result, the external characteristics and the time change rate calculated in this study are similar to those in Literature (Zhang *et al*. (2017)).

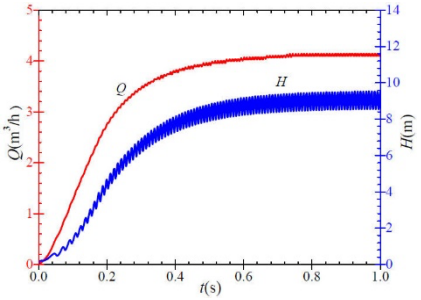

Fig. 4 Rising characteristics of head and flow

Figure 5 shows that small fluctuations occur in the flow rate increase process, which are mainly caused by dynamic and static interference. The dynamic and static interference effects cause small fluctuations in the flow during normal operation. In the current unsteady calculation of static and dynamic interference effects on steady-state problems, most constant-flow conditions are used as boundary conditions. This finding confirms that this approach is an approximate treatment, but it is acceptable. At t <0.045 s of startup, the flow rate rises slowly, which is related to the acceleration of the impeller from a standstill.

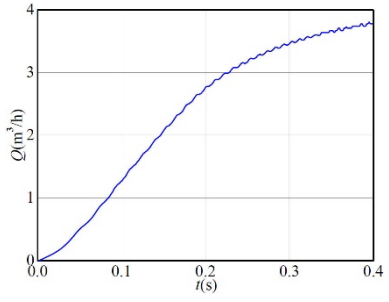

Fig. 5 Flow rising characteristics

Global Digital Central
ISSN: 2151-8629

In a radial centrifugal pump, the direction of fluid movement will change greatly, and the resulting dynamic reaction force will become an important part of the axial force. Figure 6 shows the rising process of a dynamic reaction force during startup. At t <0.1 s, the dynamic reaction force rises rapidly with a small fluctuation, and the local dynamic reaction force may be negative due to numerical calculation errors. At 0.1 s< t <0.2 s, the dynamic reaction force rises overall but fluctuates greatly. At 0.2 s< t <0.5 s, the dynamic reaction force rises steadily. At 0.5 s< t <1.0 s, the dynamic reaction force shows regular fluctuation characteristics.

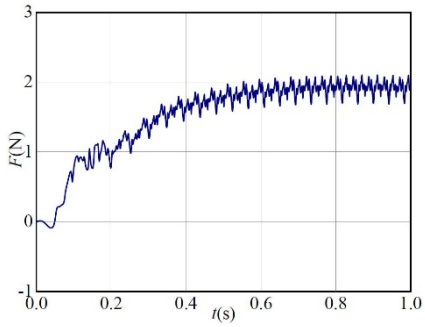

Fig. 6 Rising course of impeller dynamic reaction force

3.2 Theoretical Analysis

During the startup process, the speed rises rapidly, and rotational acceleration occurs. The flow rate increases rapidly with flow acceleration. In accordance with the generalized equation of rotary impeller machinery, the additional head during transient operation can be derived as (Chang (2005), Ping *et al*. (2007))

$$H_u = H_{u1} - H_{u2} \tag{5}$$

$$\left.\begin{aligned} H_{u1} &= \frac{\omega}{\rho g Q_d}\cdot\Omega_J\cdot D^5\cdot\frac{\mathrm{d}\omega}{\mathrm{d}t} \\ H_{u2} &= \frac{\omega}{\rho g Q_d}\cdot\Omega_M\cdot D^2\cdot\frac{\mathrm{d}Q_d}{\mathrm{d}t} \end{aligned}\right\} \tag{6}$$

where H_{u1} is the rotational acceleration head generated by the acceleration of the impeller, and H_{u2} is the fluid acceleration head consumed by the acceleration of the fluid flow inside the impeller. The two parts are called additional head. Ω_J is the rotational inertia coefficient of the flow in the impeller area, and Ω_M is the flow inertia coefficient of the flow in the impeller area.

$$\left.\begin{aligned} \Omega_J &= \frac{\pi\rho}{32}\left(\bar{D}_2^4\bar{b}_2 - \bar{D}_1^4\bar{b}_1\right) \\ \Omega_M &= \frac{\rho}{8}\left(\frac{\bar{D}_2^2}{\psi_2 tg\beta_2} - \frac{\bar{D}_1^2}{\psi_1 tg\beta_1}\right) \end{aligned}\right\} \tag{7}$$

where

$$\begin{cases} \bar{D}_1 = D_1 / D \\ \bar{D}_2 = D_2 / D \\ \bar{b}_1 = b_1 / D \\ \bar{b}_2 = b_2 / D \end{cases} \tag{8}$$

On the basis of the calculation results obtained through numerical simulation, the temporal course of the additional head during the startup process is shown in Fig. 7 and 8. At the initial moment of startup, the small flow rate causes an evident rotational acceleration head produced by the acceleration of the impeller, which then drops rapidly. The absolute value of the additional head consumed by the acceleration of the fluid in the impeller is small, and the proportion of the total additional head is small. The total instantaneous additional head drops rapidly from the larger value at the initial moment to zero, and the entire process still shows evident transient effects.

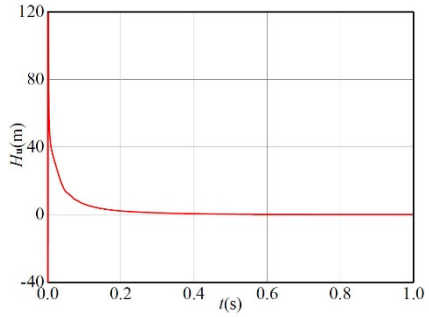

Fig.7 Rotational and fluid acceleration heads

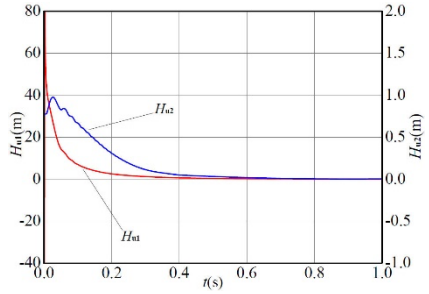

Fig. 8 Transient additional head

3.3 Flow Field Analysis

To understand and explain the transient characteristics of the startup process clearly, a quasi-steady-state calculation is conducted, and the speed is the corresponding speed. Figure 9 shows the comparison results of streamline evolution in transient and quasi-steady-state calculations in the midsection of the impeller during startup. The stable flow of this model pump at the design speed is 5 m^3/h, which is in the range of small-flow conditions. In accordance with existing research results, considerable vortex recirculation occurs inside the impeller at this time, which causes a large hydraulic loss. When t=0.02s, the corresponding speed is low, n is 181 r/min, and a complete vortex area has not yet appeared in the transient calculation; in the quasi-steady-state calculation, a complete vortex has been formed in the channel near the tongue. When t=0.06s, n is 478 r/min, in the transient calculation, a complete single-vortex structure has been formed in each flow channel and almost fills the entire flow channel; in the quasi-steady-state calculation, a complete double-vortex structure has been formed in the flow channel near the tongue. When t=0.10s, n is 705.5 r/min, the transient flow field structure and the quasi-steady flow field structure are similar to the case at t=0.06s. When t=0.14s, n is 879.8 r/min, in the transient calculation, although a large recirculation area exists in the two flow passages close to the tongue, no complete vortex structure appears there, and the only complete small vortex structure is near the exit of the far flow passage; in the quasi-steady-state calculation, a single-vortex structure exists in the two channels near the tongue, with a small vortex influence area. When t=0.20s, n is 1067.81 r/min, in the transient calculation, a vortex structure with low strength exists in the flow channel; in the quasi-steady-state calculation, a complete and strong vortex structure appears in the flow channel close to the tongue, and this phenomenon does not appear in other flow channels. When t=0.30 s, n is 1253.8 r/min, in the transient calculation, a single-vortex structure with a small influence area appears on the side of the flow channel outlet close to the pressure surface; in the quasi-steady-state calculation, a complete double-vortex structure appears in the flow channel close to the tongue, filling the entire channel. When t=0.40s, n

is 1349.3 r/min, the flow field conditions in transient and quasi-steady-state calculations are almost the same as those at t=0.30s. The difference is that the vortex intensity in the transient calculation is lower, and the influence area is smaller. When t=0.50s, n is 1398.3 r/min, the vortex and influence area in the transient calculation are minimally different from the case at t=0.40s; in the quasi-steady-state calculation, a double-vortex structure exists in the flow channel close to the tongue. One is located at the inlet with evident vortex structure, and the other is located at the outlet near the pressure surface with high strength and complete structure. At the same time, a remarkably evident and complete single-vortex structure appears in the middle of the passage that is about to turn over the tongue, but the affected area has not yet expanded. In general, the evolution of the flow field in the transient flow during the startup lags behind the calculation of the quasi-steady-state flow, which is related to the acceleration of the flow during the startup. Consequently, kinetic energy cannot be converted into pressure energy in time.

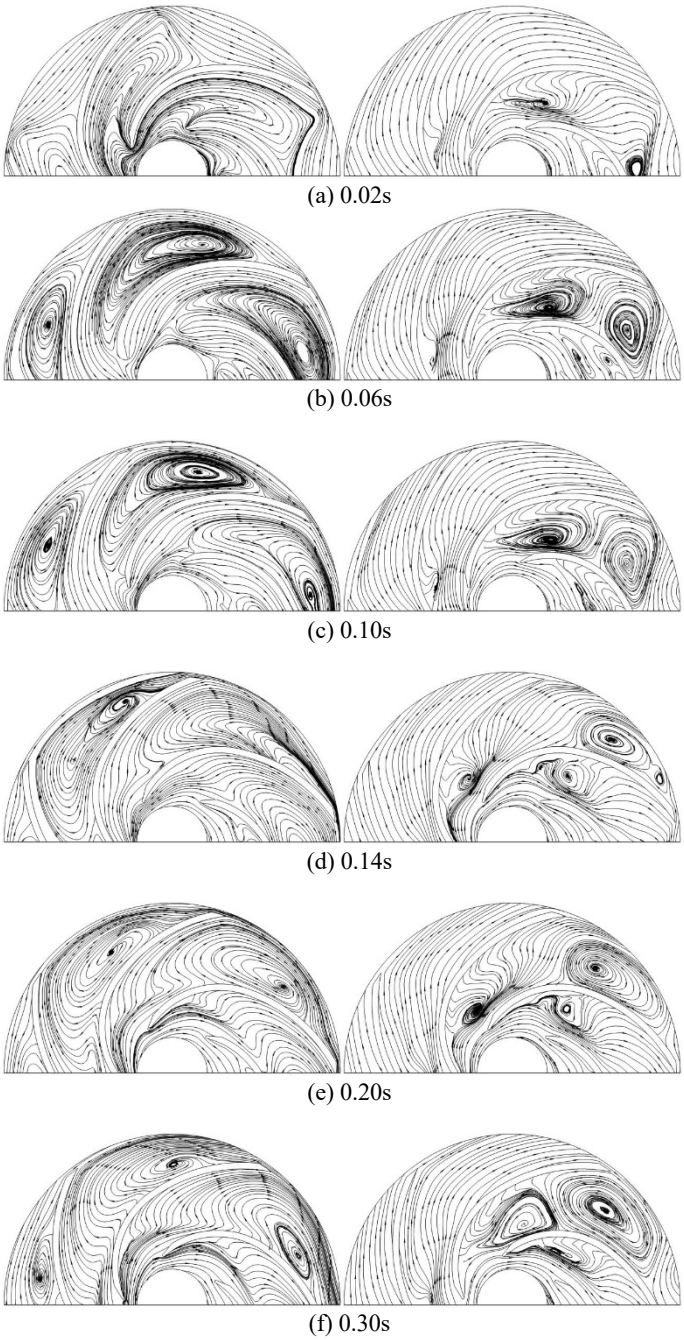

(a) 0.02s
(b) 0.06s
(c) 0.10s
(d) 0.14s
(e) 0.20s
(f) 0.30s
(g) 0.40s
(h) 0.50s
(I) Transient state (II) Quasi-steady state

Fig. 9 Comparison of transient and quasi-steady streamline evolution during startup

During the startup process, the speed accelerates sharply, resulting in a rapid increase in internal pressure. Figure 10 shows the results of the total pressure evolution at the cross-sectional position at different times during the startup process. As the speed increases, the internal pressure also shows a gradual increase trend, which is similar to the real situation. At any moment, ordinary laws exist in the pump. For example, at the same radius, the pressure on the pressure side is higher than the pressure on the suction side; the pressure gradually increases from the inlet to the outlet; the low-pressure region of the inlet makes the pump prone to cavitation. As the speed increases, the center pressure gradually decreases, and the possibility of cavitation increases. Thus, an inducer and other devices must be added in front of the impeller inlet of the high-speed pump to improve the anticavitation performance. At t>0.40 s, the speed is already extremely high, and an evident high-pressure area appears at the outlet position on the pressure surface. This high-pressure area expands with the increase in speed.

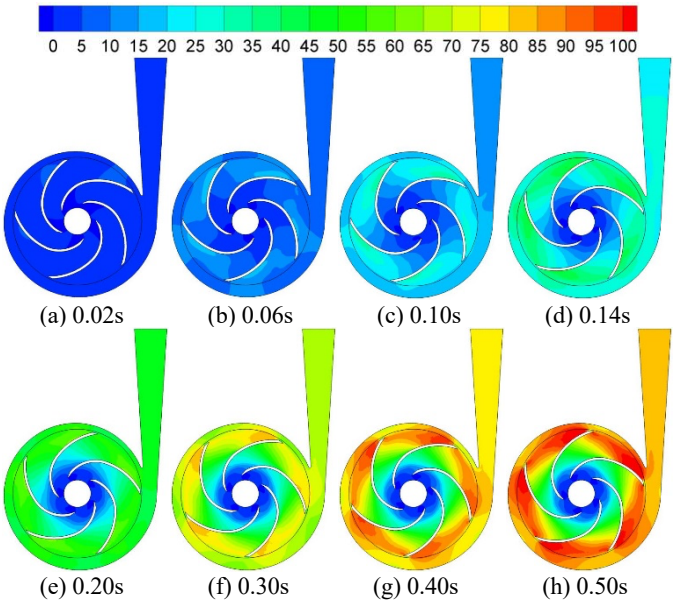

(a) 0.02s (b) 0.06s (c) 0.10s (d) 0.14s
(e) 0.20s (f) 0.30s (g) 0.40s (h) 0.50s

Fig. 10 Evolution characteristics of total pressure during startup

4 CONCLUSIONS

To eliminate the calculation errors caused by imposing boundary conditions, this study establishes a circulating closed piping system, including a centrifugal pump, which does not need to provide redundant boundary conditions for auto coupling solution. Dynamic and sliding grids are used to calculate the startup process. The results are as follows: the higher the speed is, the more evident the effect of dynamic and

static interference will be; the effect of dynamic and static interference makes the flow show small fluctuation characteristics, and the flow rate rises slowly in the initial stage; the evolution of the transient flow field lags behind that of the quasi-steady-state flow field, which may be related to the fact that the pressure energy is not converted into kinetic energy in the transient process.

ACKNOWLEDGEMENTS

The research was financially supported by the "Pioneer" and "Leading Goose" R&D Program of Zhejiang (Grant No. 2022C03170), National Natural Science Foundation of China (Grant No. 51876103), and Zhejiang Provincial Natural Science Foundation of China (Grant No. LZY21E060001 and LZY21E060002).

REFERENCES

Abed, I.M., Ali, H.F., and Sahib, S.A.M., 2020, "Investigation of heat transfer and fluid flow around sinsoudal corrugated circular cylinder for two dimensional system," *Frontiers in Heat and Mass Transfer*, 15(6), 1–9.
http://dx.doi.org/10.5098/hmt.15.6.

Chang, J.S., 2005, *Transients of Hydraulic Machine Installations*, Beijing: Higher Education Press.

Dazin, A., Caignaert, G., and Bois, G., 2007, "Transient behavior of turbomachineries: applications to radial flow pump startups," *ASME Journal of Fluids Engineering*, 129(11), 1436-1444.
https://doi.org/10.1115/1.2776963

Gu, X., Jiang, G., Wo, Y., and Chen, B., 2020, "Numerical study on heattransfer characteristics of propylene glycole-water mixture in shell side of spiral wound heat exchanger," *Frontiers in Heat and Mass Transfer*, 15(3), 1–8.
http://dx.doi.org/10.5098/hmt.15.3.

Hu, Z.Y., Wu, D.Z., and Wang, L.Q., 2005, "Transient hydrodynamic performance of centrifugal pump during rapid startup period: study of explicit characteristics," *Journal of Zhejiang University (Engineering Science)*, 39(5), 605-608, 622.
https://doi.org/10.3785/j.issn.1008-973X.2005.05.001

Lefebvre, P.J., and Barker, W.P., 1995, "Centrifugal pump performance during transient operation," *ASME Journal of Fluids Engineering*, 117(1), 123-128.
https://doi.org/10.1115/1.2816801

Li, Z.F., Wu, D.Z., Wang, L.Q., and Huang, B., 2010, "Numerical simulation of the transient flow in a centrifugal pump during startup period," *ASME Journal of Fluids Engineering*, 132(8), 1-8.
https://doi.org/10.1115/1.4002056

Ping, S.L., Wu, D.Z., and Wang, L.Q., 2007, "Transient effect annlysis of centrifugal pump during rapid startup period," *Journal of Zhejiang University (Engineering Science)*, 41(5), 814-817.
https://doi.org/10.3785/j.issn.1008-973X.2007.05.023

Tanaka, T., and Tsukamoto, H., 1999, "Transient behavior of a cavitation centrifugal pump at rapid change in operating conditions—Part1: transient phenomena at opening /closure of discharge valve," *ASME Journal of Fluids Engineering*, 121(4), 841-849.
https://doi.org/10.1115/1.2823545

Tanaka, T., and Tsukamoto, H., 1999, "Transient behavior of a cavitation centrifugal pump at rapid change in operating conditions—Part2: transient Phenomena at pump startup/shutdown," *ASME Journal of Fluids Engineering*, 121(4),850-856.
http://www.anbky.site

Tanaka, T., and Tsukamoto, H., 1999, "Transient behavior of a cavitation centrifugal pump at rapid change in operating conditions—Part3: classifications of transient phenomena," *ASME Journal of Fluids Engineering*, 121(4), 857-865.
https://doi.org/10.1115/1.2823547

Thanapandi, P., and Prasad, R., 1995, "Centrifugal pump transient characteristics and analysis using the method of characteristics," *International Journal of Mechanical Sciences*, 37(1), 77-89.
https://doi.org/10.1016/0020-7403(95)93054-A

Tsukamoto, H., and Ohashi, H., 1982, "Transient characteristics of a centrifugal pump during startup period," *ASME Journal of Fluids Engineering*, 104(1), 6-13.
https://doi.org/10.1115/1.3240859

Tsukamoto, H., Matsunaga, S., Yoneda, H., and Hata, S., 1986, "Transient characteristics of a centrifugal pump during stopping period," *ASME Journal of Fluids Engineering*, 108(4), 392-399.
https://doi.org/10.1115/1.3242594

Tsukamoto, H., Yoneda, H., and Sagara, K., 1995, "The response of a centrifugal pump to fluctuating rotational speed," *ASME Journal of Fluids Engineering*, 117(3), 479-484.
https://doi.org/10.1115/1.2817287

Wang, L.Q., Li, Z.F., Dai, W.P., and Wu, D.Z., 2008, "2-D numerical simulation on transient flow in centrifugal pump during startup period," *Journal of Engnineering Thermophysics*, 29(8), 1319-1322.
https://doi.org/10.3321/j.issn:0253-231X.2008.08.014

Wu, D.Z., Wang, L.Q., and Hu, Z.Y., 2006, "Experimental study on explicit performance of centrifugal pump during rapid startup period," *Journal of Engnineering Thermophysics*, 27(1), 68-70.
https://doi.org/10.3321/j.issn:0253-231X.2006.01.021

Wu, D.Z., Xu, B.J., Li, Z.F., and Wang, L.Q., 2009, "Numerical simulation on internal flow of centrifugal pump during transient operation," *Journal of Engineering Thermophysics*, 30(5), 781-783.
https://doi.org/10.3321/j.issn:0253-231X.2009.05.016

Wu, P., Wu, D.Z., Li, Z.F., and Wang, L.Q., 2010, "Study of transient flow in centrifugal pump during flow impulsively increase process," *Journal of Engnineering Thermophysics*, 31(3), 419-422.

Zhang, Y.L., Zhu, Z.C., Dou, H.S., Cui, B.L., Li, Y., and Zhou, Z.Z., 2017, "Numerical investigation of transient flow in a prototype centrifugal pump during startup period," *International Journal of Turbo & Jet-Engines*, 34(2), 167-176.
https://doi.org/10.1515/tjj-2015-0064